Effect of ammonia exposure and acclimation on the performance and the microbiome of anaerobic digestion

Francesc Puig-Castellví, Laëtitia Cardona, Chrystelle Bureau, Delphine Jouan-Rimbaud Bouveresse, Christophe Cordella, Laurent Mazéas, Douglas N Rutledge, Olivier Chapleur

Effect of ammonia exposure and acclimation on the performance and the microbiome of anaerobic digestion

Francesc Puig-Castellví, Laëtitia Cardona, Chrystelle Bureau, Delphine Jouan-Rimbaud Bouveresse, Christophe B.Y. Cordella, Laurent Mazéas, Douglas N. Rutledge, Olivier Chapleur

PII: S2589-014X(20)30109-2

DOI: https://doi.org/10.1016/j.biteb.2020.100488

Reference: BITEB 100488

To appear in: *Bioresource Technology Reports*

Received date: 23 June 2020

Accepted date: 23 June 2020

Please cite this article as: F. Puig-Castellví, L. Cardona, C. Bureau, et al., Effect of ammonia exposure and acclimation on the performance and the microbiome of anaerobic digestion, *Bioresource Technology Reports* (2020), https://doi.org/10.1016/j.biteb.2020.100488

Effect of Ammonia Exposure and Acclimation on the Performance and the Microbiome of Anaerobic Digestion

Francesc Puig-Castellví,[a,b] Laëtitia Cardona,[b] Chrystelle Bureau,[b] Delphine Jouan-Rimbaud Bouveresse,[c,d] Christophe B. Y. Cordella,[c,d] Laurent Mazéas,[b] Douglas N. Rutledge,[a,e] and Olivier Chapleur[b,*]

[a] Université Paris-Saclay, INRAE, AgroParisTech, UMR SayFood, 75005 Paris, France

[b] Université Paris-Saclay, INRAE, PRocédés biOtechnologiques au Service de l'Environnement, 92761 Antony, France

[c] Université Paris-Saclay, AgroParisTech, INRAE, UMR PNCA, 75005, Paris, France

[d] Research group C^2B – Chimiométrie pour la Caractérisation de Biomarqueurs

[e] National Wine and Grape Industry Centre, Charles Sturt University, Wagga Wagga, Australia

*Corresponding author: Olivier.chapleur@inrae.fr

Declarations of interest: none

Keywords: 16S rDNA sequencing, anaerobic digester, ammonia

Abstract

In this study, the effect of ammonia (NH_3) as a disturbance on the microbial communities during anaerobic digestion (AD) was examined. NH_3 was progressively added into 5 stabilized semi-continuous bio-reactors containing biowaste at 5 different NH_3 loading rates until an inhibitory concentration was reached, and maintained at this concentration for 3 hydraulic retention times (75 days). The performance and the microbial community of the digesters were analysed. The digesters performances were hindered at higher NH_3 loading rates, marked by lower biogas productions and the accumulation of volatile fatty acids. At the microbial community level, changes depended on the NH_3 loading rate. For instance, the digester with the highest NH_3 loading rate showed a hydrogenotrophic methanogenic profile resulting from the growth of *Methanosarcina spp.* and acetate-consuming microorganisms, as

well as the restricted growth of obligate acetoclastic archaea. This work can be helpful for the design of future acclimation strategies in AD.

Introduction

Anaerobic digestion (AD) is a multistep process for the treatment of organic waste that generates biogas by the action of the microorganisms. Biogas production in the anaerobic digesters strongly relies on the stability of the microbial community, which is influenced by the physicochemical state of the digester (Calusinska et al., 2018). For example, high levels of volatile fatty acids (VFA) production can inhibit methanogenesis by acidification (Garcia-Peña et al., 2011). Microorganisms can also be vulnerable to substances in the organic waste (Chen et al., 2008). In AD, the primary cause of methanogenesis inhibition is too high levels of Total Ammonia Nitrogen (TAN).

TAN is the combination of Free Ammonia Nitrogen (FAN or NH_3) and ammonium ions (NH_4^+) (Chen et al., 2008). The chemical equilibrium between TAN and NH_3 is mainly dependent on pH and temperature (Anthonisen et al., 1976). NH_3 and NH_4^+ species are commonly present in wastewater and organic waste as a result of the microbial decomposition of proteins, amino acids, uric acid and other N-containing compounds (Islam et al., 2019).

TAN inhibition power is mainly caused by NH_3. At the cellular level, NH_3 can produce an alteration of the intracellular pH, an increase in maintenance energy requirements, a depletion of intracellular potassium, and an inhibition of specific enzyme reactions (Wittmann et al., 1995). The inhibition of AD is reported to occur at a huge range of NH_3 concentrations, ranging from 27 to 1450 mg NH_3/L (Capson-Tojo et al., 2020). This can be explained by several factors, such as differences in digester operation and in the composition of the microbial communities (Capson-Tojo et al., 2020). To mitigate TAN inhibitory effects, several approaches can be used including the dilution of the reactor content with water, air

stripping, addition of absorbing material, lowering the operating temperature, co-digestion with high carbon content substrate, bioaugmentation, membrane separation, precipitate formation, addition of ion exchange media, and addition of trace elements (Bayrakdar et al., 2018; Borja et al., 1993; Farrow et al., 2017; Ortner et al., 2014; Tian et al., 2018). However, the implementation of these methods is complex and associated with high operational costs. Conversely, the acclimation of the microbial community to higher ammonia concentrations has been regarded as a practical and cost-effective strategy (Tian et al., 2018). Acclimation is a process that involves gradual adjustments within the microbial community modulated by gradual changes in their environment, improving their performance or survival (Madigou et al., 2016). Thus, in the TAN inhibition scenario, microorganisms are fed with substrate containing slowly increasing concentrations of TAN. As a result of this acclimation, microorganisms are able to tolerate TAN levels up to 5 times higher than those unacclimated (Yenigün and Demirel, 2013).

In terms of microbial assessment, previous studies investigating the TAN effect in ADs have shown that the syntrophic degraders were activated at increased TAN concentrations, while some other species as cellulolytic bacteria were inactivated (Kalamaras et al., 2020; Tian et al., 2018; Yan et al., 2019). Regarding the methanogenic community structure under the influence of TAN in ADs, discrepant results were found (Capson-Tojo et al., 2020).

The aim of this study is to elucidate how the process of microbial acclimation produces a change in the microbial community structure and, more precisely, to explore which microorganisms in the ADs can be acclimated. As well, the objective was to determine whether this change in the microbial community structure is independent of the TAN loading rate (or the time used to reach the highest TAN concentration) during acclimation. This

analysis will give insight into the observed discrepancies found in the literature about microbial inhibition due to NH_3 in ADs (Capson-Tojo et al., 2020).

To do this, anaerobic reactors were supplemented with NH_4Cl at different loading rates up to a final NH_3 concentration able to inhibit the AD process, and the microbial populations in the reactors during this acclimation process were characterized at different time-points using 16S DNA gene high-throughput sequencing. So, rather than looking at the NH_3 levels that can be reached by using the acclimation strategy as in previous studies (Kalamaras et al., 2020; Tian et al., 2018; Yan et al., 2019), in this work the effect of the time used for microbial acclimation was investigated.

In addition to this novel strategy, to our knowledge, this is the first time the system of ammonia acclimation is comprehensively studied over time at the microbial community structure level using different NH_3 acclimation times. Specifically, the sample set generated to study the microbial community evolution associated with the temporal dynamics under ammonia acclimation comprises 6 operational conditions and 8 screened time-points. In order to interpret this complex dataset, advanced chemometric methods (Bouhlel et al., 2018) were used to identify the microorganisms that responded similarly to the NH_3 acclimation process.

The outcome of this study will provide an in-depth understanding of the possible responses derived from the microbial acclimation to NH_3 during AD.

Material and methods

2.1. Feedstock and inoculum

During the course of the experiment, the bioreactor feed was prepared once a week as follows: 87 g of biowaste was diluted in biochemical potential buffer (International Standard ISO 11734 (1995)) to a final volume of 2 L to reach a concentration of 12.5 g of chemical oxygen demand per liter (COD/L). Biowaste was provided by an industrial food waste deconditioning unit (Valdis Energie, Issé, France) and kept at -20°C. Characteristics of the biowaste were as follows: dry matter = 21%, volatile matter = 92% of the dry matter, chemical oxygen demand (COD) = 287.0 gO_2/L, dissolved organic carbon (DOC) = 2704 mgC/L, dissolved inorganic carbon (DIC) = 32 mgC/L, C=50.1% of the dry matter, N=3.4% of the dry matter.

The inoculum was obtained from a mesophilic full-scale anaerobic digester treating primary sludge at the Valenton (France) wastewater treatment plant. To prepare the inoculum before its use, it was left under anaerobic conditions at 35°C for two weeks to digest the remaining residual organic matter (Cardona et al., 2019). Characteristics of the inoculum were as follows: dry matter = 1%, volatile matter = 61% of the dry matter, chemical oxygen demand (COD) = 12.9 g O_2/L, dissolved organic carbon (DOC) = 149 mgC/L, dissolved inorganic carbon (DIC) = 753 mgC/L, C=22.6% of the dry matter, N=2.2% of the dry matter.

2.2. AD experimental set-up

Six semi-continuous stirred tank reactors (Bioprocess Control AB, Sweden) with a working volume of 5 L (7 L of total reactor space) were used. Reactors were operated with a constant organic loading rate (OLR) of 0.5 g COD/L/day, a hydraulic retention time (HRT) of 25 days, an agitation of 90 rpm and at a constant temperature of 35°C. Reactor feeding was performed once a day with the previously described biowaste mixture (200 mL/day). Feeding was followed by excess liquid removal to maintain a constant volume.

The incubation consisted of 4 different periods: the initial stabilization period, the acclimation period, the plateau at the highest NH_3 concentration, and the restoration period to the initial NH_3 concentration values.

The initial period lasted for 14 weeks to stabilize the microbial communities inside the reactors. At day 98, once carbon consumption and methane production were stabilized, the process of microbial acclimation to NH_3 was started for 5 of the 6 reactors (reactors R2-R6), while the remaining reactor (R1) was left at the same stabilization conditions for the full course of the experiment. During the acclimation period, NH_4Cl (Arcos Organic, 99%) was monotonically added to the feed in reactors R2-R5, while in reactor R6, NH_4Cl was added directly. In all these digesters, the final NH_3 concentration was of 183 mg/L. This NH_3 concentration partially inhibits the microbial community, as observed in a preliminary experiment (establishment of a half inhibitory concentration for the inoculum and substrate used in this experiment as described elsewhere (Poirier et al. 2016)). The final concentration of NH_3 was reached for R2 in 3 HRT (75 days), R3 in 2 HRT (50 days), R4 in 1 HRT (25 days), R5 in 0.56 HRT (14 days), and R6 in 0.08 HRT (2 days). Thus, R1 corresponds to the control reactor, R6 to the reactor with the highest NH_4Cl loading rate, and R2 to R5 reactors covered the intermediate conditions.

The amount of NH_4Cl to be added each time to reach this NH_3 concentration was calculated after measuring the experimental values of pH and the concentration of ammonium ions (NH_4^+), and using Eqs. (1) and (2).

$$[NH_3] = \frac{10^{pH}}{(e^{\frac{6334}{T}} + 10^{pH})}[TAN], \quad \text{Eq. (1)}$$

$$[TAN] = [NH_3] + [NH_4^+], \quad \text{Eq. (2)}$$

where T represents the temperature in K, and [TAN], [NH_4^+] and [NH_3] represent respectively the final concentrations of TAN, NH_4^+ and NH_3 in mg/L.

After reaching the desired final concentration of NH_3, reactors R2-R6 were maintained at this concentration for 3 HRT (75 days). After that period, NH_4Cl addition was stopped, producing a dilution effect of the NH_3 concentration due to the addition of the feed. As a consequence, NH_3 concentration was reduced down to the initial NH_3 concentrations. A summary of the NH_3 values over the course of the experiments are given in **Figure** 1.

Temperature and pH were monitored daily. Every week, 60 mL of liquid from the reactor were collected for the chemical and microbial community structure analyses. The samples were centrifuged at 10,000 g for 10 minutes to separate the pellets from the supernatants. Both pellets and supernatants were snapped frozen in liquid nitrogen. Pellets were kept at -80°C until the DNA extraction, and supernatants were stored at -20ºC until the chemical analysis. Every week, methane content in the gas produced was measured and gas samples were collected for isotopic composition measurements.

2.3. Gas production measurements

The biogas production flow was measured using a μFlow (Bioprocess Control). The biogas was collected in Tedlar® bags and the composition was analyzed directly from the bags using a micro gas chromatograph (CP4900, Varian) as described by Madigou (Madigou et al., 2016).

In addition, gas from the digesters was sampled with 7 mL vacuumed serum tubes. The isotopic compositions of CH_4 and CO_2 ($\delta^{13}CH_4$ and $\delta^{13}CO_2$) in these samples were determined using a trace gas chromatograph Ultra (Thermo Scientific) attached to a Delta V Plus isotope ratio mass spectrometer via a GC combustion III (Thermo Scientific). $\delta^{13}CH_4$ and $\delta^{13}CO_2$ were used to establish whether methane was produced through an acetoclastic or a hydrogenotrophic methanogenesis process as in Cardona *et al.* (2019). The apparent isotopic factor (α_{app}) was calculated from $\delta^{13}CH_4$ and $\delta^{13}CO_2$ with the following equation:

$$\alpha_{app} = (\delta^{13}CO_2 + 10^3) / (\delta^{13}CH_4 + 10^3) \quad \text{Eq. (2)}$$

It is conventionally assumed that if α_{app} is higher than 1.065, methane was mainly produced through the hydrogenotrophic pathway. On the other hand, if α_{app} is lower than 1.055, methane was produced through the acetoclastic pathway (Conrad, 2005; Whiticar et al., 1986).

2.4. Chemical analysis

Acetic acid, butyric acid, and propionic acid were quantified in an ionic chromatograph (ICS 5000+, Thermo Fisher Scientific) equipped with an IonPAC ICE-AS1 column and using a mobile phase composed of heptafluorobutyric acid (0.4 mmol/L) and tetrabutylammonium (5 mmol/L).

Ammonium ion (NH_4^+) concentration was determined using the Nessler's colorimetric method following the French norm (NF T 90-105) (Cardona et al., 2019), and the dissolved organic and inorganic carbons were measured following the French norm NF EN 1484 using a DOC analyzer (TOC-L-Shimadzu).

2.5. Microbial structure analysis

For each reactor, the 16S DNA was sequenced for 8 samples (days 84 (before acclimation), 98 (start of acclimation), 105, 112, 133, 154, 182 and 217). This sampling aimed to determine the evolution of the microbial communities during the period of acclimation to NH_3.

Total DNA was extracted from the pellet using Powersoil™ DNA isolation kit (Mobio Laboratories Inc. Carlsbad) according to the manufacturer's instructions. Extracted DNA concentrations were determined using a quantifying fluorescent dye assay (Qubit dsDNA HS Assay Kit, Invitrogen, Eugene) and Qubit 2.0 Fluorometer (Invitrogen, Life Technologies, Eugene).

The DNA extracted by this method was used for the amplification of the bacterial and archaeal hypervariable region V4–V5 of the 16S rDNA genes with the primers 515F (5′-GTGYCAGCMGCCGCGGTA-3′) (Wang et al., 2007) and 928R (5′-CCCCGYCAATTCMTTTRAGT-3′) (Wang and Qian, 2009). More precisely, a fusion method was employed (IonAmplicon Library Preparation (FusionMethod) Protocol, Revision C). The forward primer was modified by the addition of a PGM sequencing adaptor (adaptor A: 5′-CCATCTCATCCCTGCGTGTCTCCGACTCAG-3′) and a barcode (5′-adaptor A-Barcode-515F-3′). The reverse primer was modified by the addition of a PGM sequencing adaptor (adaptor trP1: 5′-CCTCTCTATGGGCAGTCGGTGAT-3′) (5′-adaptor trP1-928R-3′). V4–V5 region was amplified according Platinum Pfx Supermix protocol (Life Technologies) in a 50 µL reaction mixture containing 1X Pfx amplification buffer, 0.3 mM dNTP mix, 1 mM $MgSO_4$, 0.3 µM of each primer, 1U of PlatinumPfx DNA polymerase, and 10-20 ng extracted DNA. The mixture was held at 94 °C for 5 min, followed by 30 cycles at 94 °C for 15 s, 50 °C for 30 s and 68 °C for 1 min, and a final extension step at 68 °C for 5 min.

PCR products were cleaned using the Agencourt AMPure XP magnetic beads purification system (Beckman Coulter) according to the manufacturer's instructions, with a bead:amplicon ratio of 1.2, and were eluted in 45 µL TE Buffer (10 mM Tris-HCl pH 8.0, 1 mM EDTA). Quantification was done with a capillary electrophoresis bioanalyzer (2100 Electrophoresis Bioanalyzer, Agilent Technologies, Santa Clara) using the Agilent DNA 1000 Kit (Agilent Technologies). Purified libraries were diluted (in a first step to 500 pM and then to 100 pM). Equal volumes of amplicons were then combined in equimolar concentrations (100 pM) for sequencing. Emulsion PCR was carried out to prepare template-positive ISPs containing clonally amplified DNA, using the Ion PGM™ Hi-Q View OT2 Kit with the Ion OneTouch™ 2 Instrument. The template-positive ISPs were enriched with the Ion OneTouch™ ES according to the manufacturer's instructions. Sequencing was performed on

an Ion Torrent Personal Genome Machine using Ion 316 chip and the Ion PGM Hi-Q View Sequencing Kit according to the manufacturer's instructions. The PGM software filtered out low quality and polyclonal sequence reads, and the quality filtered data was exported as FastQ file. Between 10,000 and 40,000 high quality reads were generated for each sample.

2.6. Bioinformatic analysis

The FROGS pipeline was used to analyze the 16S DNA tags reads. FROGS (Find Rapidly Operational Taxonomic Units (OTU) with Galaxy Solution) is a galaxy workflow designed to produce an OTU count matrix from high depth sequencing amplicon data (Escudié et al., 2018). Briefly, the reads between 100 and 500 base pairs (bp) were merged and the resulting dataset was denoised. The reads kept were clustered with Swarm algorithm, and chimera and singleton reads were removed. Finally, the taxonomic affiliation of the remaining reads was determined using Silva132 16S as the reference database, resulting in 1287 different OTUs. The counts for every sample and OTU were arranged into a 48-by-1287 data matrix (samples in rows, OTU counts in columns).

2.7. Data analysis pipeline

OTU counts were analyzed using both traditional and advanced data analysis methods.

In the first approach, the microbial community structure in the reactors was investigated with bar plots of their relative abundances (Puig-Castellví et al., 2020) built using the *phyloseq* R-package (McMurdie and Holmes, 2013). The tolerance to NH_3 was investigated at the order level for the bacterial populations and at the genus level for the archaeal populations.

In the second approach, with the aim of getting a better understanding of the microbial dynamics across reactors and time, while maintaining the full affiliation of the microorganisms, the same data were examined using chemometric methods. In this approach, every sample was first normalized by the Relative Log Expression method (Anders and

Huber, 2010; Badri et al., 2018) using the *scone* R-package (Cole and Risso, 2019). Next, OTUs not present in at least 20 % of the samples were discarded to reduce the dataset sparsity. Doing this, 703 OTUs were kept for further analysis. Before removal of the discarded OTUs, the randomness of their distribution in relation to the experimental setup was checked, and it was concluded that their presence could not be attributed to the ammonia addition.

The resulting OTU counts data matrix was investigated by Common Components Analysis (CCA) (Bouhlel et al., 2018; Puig-Castellví et al., 2020; Rutledge, 2018). CCA searches for orthogonal components defined by a linear combination of the original variables, as in Principal Component Analysis (PCA). However, CCA has the advantage over PCA in that variables that have the same effect on the dispersion of the observations will be grouped together in the same Common Component (CC), and that the first CCs will group together the largest number of variables with the greatest effect on a particular dispersion of the individuals. In CCA, each component is composed of a scores vector (the coordinates of the sample on the orthogonal directions in the CC subspace), a loadings vector (the contributions of the original variables to the definition of the new subspace directions), and a salience vector (corresponding to the importance of the variables in defining each CC direction).

In this analysis, CCA was used to determine those OTUs that presented a similar response to the ammonia acclimation period across the different reactors. Data were column-centered and norm-scaled before CCA (Bylesjö et al., 2009). For each CC, variables (*e.g.*, OTUs) associated with loading values beyond 2 standard deviations ($\pm 2 \times SD$) were selected (Bouhlel et al., 2018) and graphically represented in a topological tree based on the phylogenetic data of these OTUs using the GraPhlAn online tool from the Galaxy website (http://huttenhower.sph.harvard.edu/galaxy/).

Results and discussion

1) Bioreactor performance

Figure 1 shows the chemical performance data (biogas production, methane concentration, α_{app}, pH, volatile fatty acids acetate and propionate concentrations, DOC, and DIC), as well as the NH_3 concentration, for the different reactors over the course of the experiment.

Results from **Figure1** show that the stabilization phase (which lasted until the 98th day) had a similar behaviour in all reactors. In general, the biogas production was around 400 mL/day and contained 85% of methane. Moreover, the methanogenic profile observed during the stabilization phase was acetoclastic (α_{app} < 1.055). The value of the NH_3 concentration stabilized at approximately 20 mg/L, which is insufficient to cause inhibition (Capson-Tojo et al., 2020). The lack of inhibition was confirmed by the absence of VFAs accumulation and the pH constant at around 7.8. A deviation from the general performance was detected for the biogas production in R4, which was at 350 mL/day. This lower gas production was attributed to a gas leakage during stabilization. This hypothesis is supported by the fact that the rest of the parameters for R4 were comparable to those of the other reactors.

During the acclimation period, the relative CH_4 content remained stable although the biogas production dropped at a rate proportional to the NH_3 addition rate. This response suggests that the methanogenic community was strongly affected by the NH_3 addition. This is in agreement with the fact that acetoclastic methanogens are considered to be the microorganisms most sensitive to NH_3 excess (Rajagopal et al., 2013).The DOC and the acetate levels increased, while the DIC decreased. This response suggests a reduced microbial activity from the species involved in the last steps of the degradation. Propionate levels also increased in the digesters with the shortest NH_3 acclimation period. The rest of the parameters followed the same profile observed during the stabilization phase.

During the plateau at the highest NH_3 concentration (represented in **Fig1** by the two lines of the same color as the reactor label), some parameters varied more significantly.

At the beginning of the plateau, when ammonia level was maximum in the reactors, the lowest biogas production was observed for every reactor. This time-point also presented the maxima of DOC and the minima of DIC. In addition, for reactors R5 and R6, and to a lesser extent in reactor R2, it coincides with the minimal relative content of CH_4 in the biogas. For R3 and R4, the relative content of CH_4 remained unaffected. After this low biogas production, the values were partially restored later. The time needed for the recovery of the gas production was longer for those digesters with the faster NH_3 addition (R5 and R6).

The methanogenic activities during the early part of the plateau period shifted towards the hydrogenotrophic profile due to the NH_3 addition, and were shifted back to acetoclastic after the biogas production was restored. The observed minima value of DIC could be a consequence of the assimilation of the dissolved CO_2 by hydrogenotrophic archaea. However, the only digester that was effectively hydrogenotrophic (α_{app} higher than 1.065) at some point during the plateau period was R6. For R2-R5 reactors, the calculated α_{app} values indicated mixed contributions of both acetoclastic and hydrogenotrophic methanogenesis.

In all the altered reactors (R2-R6), the increase of the NH_3 levels caused an accumulation of VFA (acetate and propionate) that reached their maxima at the plateau period (**Fig. 1**) revealing some degree of inhibition caused by the NH_3 addition Hence, the high values of DOC may be representative of this VFA accumulation. However, after that maxima, the VFA decreased in all digesters except for the one with the immediate NH_3 addition. This result indicates that despite all digesters being altered due to the NH_3 addition, the acclimation strategy in R2-R5 reactors allowed for a faster recovery than in R6. Derived from the accumulation of VFA, the pH during the plateau in R6 was more acid than in the other reactors (**Fig.1**). Similarly, for R5, the pH was also slightly more acidic, although it returned

to normal values by the end of the plateau. In reactors R2-R4, pHs were close to those in R1, indicating that the reactor conditions were more stable in those reactors in which NH_3 was added more slowly.

Finally, the decrease in the NH_3 concentration after the plateau did not modify the biogas production (except for R3, where it decreased), nor the relative content of methane, VFAs, DOCs and DICs compared to the end of the plateau. On the other hand, the decrease in NH_3 caused a basification of the pH (the change is most apparent in R2), and digesters R3 and R6 showed a methanogenic hydrogenotrophic activity. The higher variability in terms of pH and methanogenic activity across digesters in this last period can be argued as the recovery of the original NH_3 levels resulted in a less constrained environment in ecological terms. Then, the observed differences across digesters are the consequence of the stochastic readjustment of the microbial community to the new NH_3 concentration levels.

2) Relative abundance in the reactors

Overall, the microbial diversity consisted of 1287 OTUs (34 archaeal OTUs and 1253 bacterial OTUs). Of these, 91 OTUs (5 archaeal OTUs and 86 bacterial OTUs) had a relative abundance greater than 1% in at least one of the samples.

The archaeal diversity (**Fig.2A**) is mainly dominated by the methanogenic archaea *Methanobacterium* (1 OTU) and *Methanosarcina* (2 OTUs).

At the 84^{th} day, the sample point descriptive of the stabilization period, the relative abundance of the total archaea in R1-R6 reactors was 2.3-3.9%. Similarly, in the reactor with no NH_3 addition (R1), the archaeal diversity remained steady during all the experiment and the relative abundance of the total archaea was <3%. In reactors with slow NH_3 addition (R2-R5), the archaeal structure was similar to that of R1, but less stable over time. However,for the reactor with the fastest NH_3 addition (R6), the archaeal population total relative

abundance decreased continuously during the plateau until the 133th day, implying that the NH_3 exposure was too intense to allow the survival of the community.

In R6 and to a lesser extent in R5, coinciding with the lowered NH_3 levels at the latest time-points, the archaea levels rose to >8% of the relative abundance. The substantial increase of the archaea population was mainly associated with one *Methanosarcina spp.* (OTU_11). Thus, the increase of *Methanosarcina* relative abundance after lowering the NH_3 levels must be regarded as an adaptation response to the acclimation period since these relative abundance values are much higher than those found in the control reactor (R1), despite the NH_3 values in R5 and R6 reactors being higher (~150 mg/L) at the latest dates. *Methanosarcina* is known to be more tolerant to ammonia inhibition than other archaea (Bonk et al., 2018). It must be noted, however, that the relative abundance of *Methanosarcina* dropped in R6 reactor at day 217 (at the restoration period). This decrease was interpreted to be the result of the removal of the environmental pressure to the inhibited microorganisms, which can now recover their initial niche, and to the consumption of an important quantity of accumulated VFA facilitating archaea growth (**Figure1**).

The bacterial structure of the reactors was composed of more than 24 orders, *Bacteroidales* (31 OTUs), *Cloacimonadales* (4 OTUs), *Clostridiales* (23 OTUs) and *Synergistales* (4 OTUs) being the predominant ones (**Fig.2B**).

Analogously to the archaeal structure, the bacterial structure at the 84th day was very similar across reactors, denoting their successful stabilization.

The bacterial profile of R1 remained very stable over time, although some changes in diversity were detected. For instance, one *Sphingobacteriales* species (OTU_22) reached observable abundances at day 105 (**Fig. 2B**), and persisted during the rest of the experiment.

Two distinct bacterial dynamics depending on the NH_3 addition rate were observed.

The first was observed for R2-R5 reactors. In these reactors, *Cloacimonadales* were more prominent than in R1, although their presence was severely hindered in R5 at 182nd and 217th days (end of plateau and restoration periods, respectively) (**Fig2B**). This decrease seems to be connected to the recovery of *Methanosarcina* population for the same samples (**Fig2A**). *Cardiobacteriales* (1 OTU), *DTU014* (1 OTU), *Izimaplasmatales* (1 OTU), and *Spirochaetales* (3 OTUs) also presented significant abundances in reactors R2-R5 compared to R1. These microorganisms, together with the archaeon *Methanosarcina*, should be regarded as the ones most acclimatable to NH_3.

The second microbial dynamic was observed in reactor R6. Firstly, by day 112th (at the start of the plateau period), *Cloacimonadales* relative abundance became negligible. In line with the response observed for reactors R2-R5, it can be interpreted that *Cloacimonadia spp.* does not tolerate a fast increase in the NH_3 levels. Secondly, at later time-points in R6, *Spirochaetales* (3 OTUs) and *Acholeplasmatales* (1 OTU) had a substantial increase, and to a lesser extent, also *DTU014* (1 OTU), *Enterobacteriales* (4 OTUs), and *MSBL9* (1 OTU), among others. This fact indicates that these microorganisms are highly tolerant and can grow despite the high ammonia concentration. The low relative abundances of *Cardiobacteriales* and *Izimaplasmatales* in R6 suggests that these two microorganisms can only be acclimated if NH_3 is added slowly.

The different temporal fluctuations observed in the reactors revealed that the microbial susceptibility to NH_3 is very complex and varies among microorganisms.

3) Microbial Response to NH_3

In order to get a general view of the dynamics of the microbial communities across reactors and time, and untangle the main growing responses to NH_3, the microbial data were analyzed with CCA (**Figure 3A-C**). In this analysis only those OTUs that were detected in at

least 20% of the samples (n=703 OTUs, see *Methods*) were considered. With CCA, the components obtained are a linear combination of the OTUs that give the same dispersion for the set of samples. Thus, CCA detects those OTUs that have a similar susceptibility to NH_3, even if these OTUs are found at subdominant population levels. Moreover, the most significant OTUs for each component can be regarded as representative of the main microbial community dynamics (see *Methods*) and are discussed more in detail below.

CCA only revealed three interpretable components, and the CCA scores are given in **Fig3A-C**.

The temporal evolution of the scores in Common Component 1 (CC1, **Fig3A**) show that the most important microbial community alteration is the inhibition that appeared after the start of NH_3 addition at day 98. In this component, score values slowly declined over time for reactor R1 samples. For reactor R2-R6 samples, the same trend was observed during the first half of the experiment, although the scores declined more steeply and reaching negative values after day 112. CC1 is therefore descriptive of a microbial community prevalent in R1 and inhibited in reactors R2-R6 at 183 mg/L of NH_3. It is worth noting that, in reactors R2-R5, the microbial community represented by this component shows a partial tolerance to NH_3, since it was not strongly inhibited until it was exposed to the highest NH_3 concentrations.

On the other hand, both Common Component 2 (CC2, **Fig3B)** and 3 (CC3 (**Fig3C**, respectively) were mainly representative of the microbial dynamics within just one of the reactors. Specifically, these reactors correspond to those with the two fastest NH_3 addition rates (CC2 for R5, and CC3 for R6). For these two reactors, the temporal evolution of CC2 and CC3 peaked at the 154^{th} and 105^{th} days, respectively, both coinciding with two samples from the stabilization plateau. Thus, the exposure to short acclimation periods caused two different changes in the microbial community composition (one observed in reactor R5 and the other in reactor R6).

However, while the whole acclimation period in R5 was mainly defined by CC2, CC3 was only relevant during the first half of the corresponding acclimation period in R6. This result reveals that the microbial community represented by CC3 was not stable over time and died after circa 1.5 HRT, and led to a switch of the methanogenic profile towards hydrogenotrophic methanogenesis. This disturbance could be due to the abrupt acidification (**Fig1** and **Fig3E**). Hence, NH_3 additions similar to those used in R6 must be avoided so as to not produce microbiota instabilities.

Furthermore, CC2 also showed a mild contribution in reactor R3 during the acclimation period, although this contribution disappeared when the highest NH_3 concentration was reached. This result suggests that the microbial community defined by CC2 can only exist while the non-acclimatable microorganisms are inhibited. This was also observed in reactor R5, since CC2 contribution decreased significantly during the NH_3 restoration period.

Finally, the fact that none of the components showed positive scores during the plateau period in R2-R4 reactors points out that the NH_3 acclimation in those reactors did not require a strong readjustment of the microbial community, but it was mediated instead by physiological changes in the microorganisms.

To summarize, we can conclude than CC1 is representative of the microbial community that is inhibited by NH_3 addition, while CC2 and CC3 correspond to those that can survive the acclimation period. At the same time, microorganisms represented by CC3 can tolerate higher levels of NH_3 than those represented by CC2 (**Figure 4**).

4) Key microorganisms of the NH_3 acclimation

In order to focus on the most characteristic OTUs from each CC, only the OTUs with high loadings (greater than ± 2 SD) were selected and used for microbial interpretation.

Hence, 13 OTUs were selected for CC1, 45 OTUs for CC2, and 47 for CC3. In total, 103 OTUs (4 archaeal and 99 bacterial) were selected in at least one CC.

All 4 selected archaea belong to different families (*Methanobacteriaceae*, *Methanosarcinaceae*, *candidatus Methanomethylophilaceae*, and to an unknown family from the phylum *Crenarchaeota*), whereas the bacteria are from 27 different orders (see **Supplementary Table S1**).

OTUs selected in CC1 are from diverse orders, indicating that the inhibitory action of NH_3 is prevalent across all microbial realms. These OTUs, from *Aminicenantia*, *Anaerolineae*, *Coprothermonbacteriales*, and *Cloacimonadales* among others, are typical from sewage sludge (Rivière et al., 2009). The inhibition (and lack of adaptation) of these OTUs due to NH_3 may result from the absence of mechanisms for surviving at high NH_3 levels, which would be unnecessary for these OTUs since NH_3 concentration in sludge is typically not as elevated. Similarly, *Crenarchaeota*, a chemolitoautotroph archeon that grows by oxidizing NH_3 (Könneke et al., 2005), was also selected in CC1. It can be argued that the inhibition of this microorganism results from the unsuitable environmental conditions for carrying out the NH_3 oxidation, as ammonia-oxidizing archaea prefer soils with low NH_3 levels (Di et al., 2010).

Conversely, the presence of OTUs from polyphyletic classes, such as *Clostridia* or *Bacteroidales*, is reduced in this component pointing out the preference of these microorganisms for N-enriched environments as reported elsewhere (Rui et al., 2015).

Finally, methanogenic archaea were not selected in CC1 despite it being known that they are inhibited in NH_3 rich environments (Yenigün and Demirel, 2013), suggesting that these microorganisms successfully adapted to NH_3 inhibition. This can be observed in **Fig2** for *Methanosarcina* (with an increased abundance at the latest time-points in reactors R5 and R6) and *Methanobacterium* (since similar abundance levels were maintained throughout the

experiment). Regarding CC2, a wide range of microorganisms was selected. Most of the selected OTUs (except for OTU_59) are associated with a better growth during the stabilization plateau in reactor R5. On the other hand, the response was severely inhibited for OTU_59 (genus *Acetobacteroides*). The only species reported from this genus is an acetate- and hydrogen-producer (Su et al., 2014). In this experiment, the highest acetate concentration was found in reactor R5 shortly after the start of the plateau (day 133). Thus, it is possible that inhibition of OTU_59 growth is due to acetate accumulation.

In CC2, 2 archaea were selected. One is a hydrogenotrophic *Methanobacteriaceae* (OTU_38), while the other is a *Methanomethylophylaceae* (OTU_210) capable of using methyl-amine as substrate for methane formation (Borrel et al., 2017). It has been reported that *Methanobacteriaceae* are hardly affected by NH_3 inhibition (Bonk et al., 2018). The existence of hydrogenotrophic archaea in this component would also explain the peak in the apparent isotopic factor observed in reactors R3 and R5 after entering into the acclimatisation plateau. On the other hand, methyl-amine formation may be favoured in ammonia-rich environments (such as the in these reactors), thus promoting the growth of *Methanomethylophylaceae* species.

As for the bacterial OTUs selected in CC2, the most numerous phylogenetic orders are the *Clostridiales* (19 OTUs), *Bacteroidales* (8 OTUs) and *Synergistales* (5 OTUs). *Clostridales*, together with *Bacteroidales*, showed an increased relative abundance due to NH_3 concentration (De Vrieze et al., 2015), while *Synergistales* can grow in environments rich in NH_3 (Godon et al., 2005).

Within the *Clostridiales*, the most important families were *Family XI (5 OTUs)*, *Family XIII (3 OTUs)*, *Ruminococcaceae (3 OTUs)* and *Syntrophomonadaceae (5 OTUs)*. *Syntrophomonas* have been described as NH_3-tolerant (Bonk et al., 2018). In addition, *Tissierella* (from *Family XI*) presence is known to be enhanced by the thermal hydrolysis of

amino acids in sewage sludge, which is a NH_4^+-releasing chemical process (Chen et al., 2019).

Finally, in this component, a *Spirochete* OTU was also selected. Nevertheless, in this case, its favorable growth in R5 could be attributed to its ability to consume acetate (Lee et al., 2015), such as *Syntrophomonas*.

CC3 is descriptive of the microbial community resistant to a fast NH_3 addition (**Fig3C**). The highest level of this component is found in reactor R6, coinciding with the start of the NH_3 addition, indicating a marked preference for N-enriched media.

Only a *Methanosarcina mazei* archaea species was selected in CC3 while for bacteria, the major groups are the *Clostridiales* (26 OTUs) and the *Bacteroidiales* (8 OTUs). In addition, single OTUs from the bacterial orders *Alphaproteobacteria*, *Bacilli*, *Desulfovibrionales*, *Erysipelotrichia*, and *Phycisphareae*, among others, were also selected in CC3 (**Fig.3**).

Most of the OTUs from *Clostridiales* and *Bacteroidales* were selected either in CC2 or CC3 component, showing that OTUs from these two groups have a preference for the presence of NH_3 (De Vrieze et al., 2015).

Within the *Bacteroidales*, the most common genus was *Proteiniphilum* (5 OTUs). Interestingly, in a recent publication, *Proteiniphilum* growth was found to be promoted by the thermal hydrolysis of proteins, which could be a source of NH_3 (Chen et al., 2019).

Within the *Clostridiales*, the most common families were *Clostridiaceae 1* (5 OTUs), *Christensenellaceae* (4 OTUs), *Ruminococcaceae* (4 OTUs), *Lachnospiraceae* (3 OTUs) and *Peptostreptococcaeae* (3 OTUs).

On the other hand, two OTUs (OTU_17 and OTU_65, a *Synergistales* and a *Betaproteobacteriales*) were selected for both CC2 and CC3, revealing the capability of some

microorganisms to adapt differently in presence of high NH_3 levels depending on the addition rate.

Interestingly, some of the OTUs selected for CC3 are known to play a role in the microbial community rearrangement derived from the TAN addition with no acclimation in batch AD reactors (Poirier et al., 2016). For instance, the archaeon *Methanosarcina mazei* was the predominant archaeon when TAN levels were increased to 7.5g/L in Poirier's study (Poirier et al., 2016). In addition, in that study, *Ruminococcaceae* and *Lachnospiraceae* (among other *Clostridia*) were found to be predominant in reactors with low initial TAN levels (up to 10g/L), while *Peptostreptococcaeae* was associated with 25g/L TAN. Furthermore, OTU_17 and OTU_65 were found to respond positively when extreme concentrations of TAN (up to 50g/L) were used.

The fact that no obligate acetoclastic methanogen was selected in CC3 can be explained by acetoclastic archaea being more sensitive to NH_3 than the hydrogenotrophic archaea (Borja et al., 1996). It has also been stated that *Methanosarcina* species are more resistant to high NH_3 levels than other methanogenic archaea because of their high volume to surface ratio and to their capability to form big clusters (Calli et al., 2005). Moreover, the switch from acetoclastic methanogenesis to hydrogenotrophic methanogenesis (**Fig3F**) may have also been strengthened by the growth of bacteria that perform symbiosis or syntrophic relationship with hydrogenotrophic bacteria, such as the sulfate-reducing *Desulfovibrio* (Bryant et al., 1977), the H_2-producing *Acetivibrio* (Patel and MacKenzie, 1982), and the acetate-oxidizing *Synergistaceae* (Ito et al., 2011), all of which are selected in CC3. In all, this explains the accumulation of acetate in reactor R6 (**Fig. 1**).

The marked hydrogenotrophic profile of the microbial community described by CC3 was also observed experimentally (**Fig. 3F**). While reactors R1-R5 presented an acetoclastic profile over the whole course of the experiment, R6 followed a different trend, switching to a

hydrogenotrophic profile after the addition of NH_3 (day 98) and peaking at day 133 (**Fig. 3F**). After the acclimation period was finished, the methanogenic profile transitorily switched back to acetoclastic and then returned again to hydrogenotrophic at the last sampled day, indicating that the acclimated microbial community was in overall hydrogenotrophic.

This observed instability of the methanogenesis profile agrees with the fact that the microbial community defined by CC3 did not last for all the stabilization plateau in R6 (**Fig3C**).

Conclusions

The strategy of NH_3 acclimation caused perturbations in the performance of all digesters, the one from the digester with the fastest NH_3 addition being the most extreme.

CCA revealed 3 main changes in the community structure derived from the NH_3 addition, associated with the inhibition of non-acclimated microorganisms and the growth of the acclimated ones. Most of these microorganisms belonged to the orders *Clostridiales* and *Bacteroidales*.

Hence, we have shown that the AD process can be acclimated to NH_3, and that the resulting changes in the microbial community structure will be a function of the NH_3 concentration and addition rate.

Acknowledgements

This work is supported by the French ANR project DIGESTOMIC (ANR-16-CE05-0014).

References

Anders, S., Huber, W., 2010. Differential expression analysis for sequence count data. Genome Biol. 11, R106. https://doi.org/10.1186/gb-2010-11-10-r106

Anthonisen, A.C., Loehr, R.C., Prakasam, T.B., Srinath, E.G., 1976. Inhibition of nitrification by ammonia and nitrous acid. J. Water Pollut. Control Fed. 48, 835–52.

Badri, M., Kurtz, Z.D., Müller, C.L., Bonneau, R., 2018. Normalization methods for microbial abundance data strongly affect correlation estimates. bioRxiv 406264. https://doi.org/10.1101/406264

Bayrakdar, A., Sürmeli, R.Ö., Çalli, B., 2018. Anaerobic digestion of chicken manure by a leach-bed process coupled with side-stream membrane ammonia separation. Bioresour. Technol. 258, 41–47. https://doi.org/10.1016/j.biortech.2018.02.117

Bonk, F., Popp, D., Weinrich, S., Sträuber, H., Kleinsteuber, S., Harms, H., Centler, F., 2018. Ammonia Inhibition of Anaerobic Volatile Fatty Acid Degrading Microbial Communities. Front. Microbiol. 9, 2921. https://doi.org/10.3389/fmicb.2018.02921

Borja, R., Sánchez, E., Weiland, P., 1996. Influence of ammonia concentration on thermophilic anaerobic digestion of cattle manure in upflow anaerobic sludge blanket (UASB) reactors. Process Biochem. 31, 477–483. https://doi.org/10.1016/0032-9592(95)00099-2

Borja, R., Sánchez, E., Weiland, P., Travieso, L., 1993. Effect of ionic exchanger addition on the anaerobic digestion of cow manure. Environ. Technol. (United Kingdom) 14, 891–896. https://doi.org/10.1080/09593339309385362

Borrel, G., McCann, A., Deane, J., Neto, M.C., Lynch, D.B., Brugère, J.-F., O'Toole, P.W., 2017. Genomics and metagenomics of trimethylamine-utilizing Archaea in the human gut microbiome. ISME J. 11, 2059–2074. https://doi.org/10.1038/ismej.2017.72

Bouhlel, J., Jouan-Rimbaud Bouveresse, D., Abouelkaram, S., Baéza, E., Jondreville, C., Travel, A., Ratel, J., Engel, E., Rutledge, D.N., 2018. Comparison of common components analysis with principal components analysis and independent components analysis: Application to SPME-GC-MS volatolomic signatures. Talanta 178, 854–863.

https://doi.org/10.1016/J.TALANTA.2017.10.025

Bryant, M.P., Campbell, L.L., Reddy, C.A., Crabill, M.R., 1977. Growth of desulfovibrio in lactate or ethanol media low in sulfate in association with H2-utilizing methanogenic bacteria. Appl. Environ. Microbiol. 33, 1162–1169.

Bylesjö, M., Cloarec, O., Rantalainen, M., 2009. Normalization and Closure. Compr. Chemom. 109–127. https://doi.org/10.1016/B978-044452701-1.00109-5

Calli, B., Mertoglu, B., Inanc, B., Yenigun, O., 2005. Community changes during start-up in methanogenic bioreactors exposed to increasing levels of ammonia. Environ. Technol. 26, 85–91. https://doi.org/10.1080/09593332608618585

Calusinska, M., Goux, X., Fossépré, M., Muller, E.E.L., Wilmes, P., Delfosse, P., 2018. A year of monitoring 20 mesophilic full-scale bioreactors reveals the existence of stable but different core microbiomes in bio-waste and wastewater anaerobic digestion systems. Biotechnol. Biofuels 11, 196. https://doi.org/10.1186/s13068-018-1195-8

Capson-Tojo, G., Moscoviz, R., Astals, S., Robles, Steyer, J.P., 2020. Unraveling the literature chaos around free ammonia inhibition in anaerobic digestion. Renew. Sustain. Energy Rev. https://doi.org/10.1016/j.rser.2019.109487

Cardona, L., Levrard, C., Guenne, A., Chapleur, O., Mazéas, L., 2019. Co-digestion of wastewater sludge: Choosing the optimal blend. Waste Manag. 87, 772–781. https://doi.org/10.1016/J.WASMAN.2019.03.016

Chen, S., Dong, B., Dai, X., Wang, H., Li, N., Yang, D., 2019. Effects of thermal hydrolysis on the metabolism of amino acids in sewage sludge in anaerobic digestion. Waste Manag. 88, 309–318. https://doi.org/10.1016/J.WASMAN.2019.03.060

Chen, Y., Cheng, J.J., Creamer, K.S., 2008. Inhibition of anaerobic digestion process: A review. Bioresour. Technol. 99, 4044–4064. https://doi.org/10.1016/J.BIORTECH.2007.01.057

Cole, M., Risso, D., 2019. scone: Single Cell Overview of Normalized Expression data. https://doi.org/10.18129/B9.bioc.scone

Conrad, R., 2005. Quantification of methanogenic pathways using stable carbon isotopic signatures: a review and a proposal. Org. Geochem. 36, 739–752. https://doi.org/10.1016/j.orggeochem.2004.09.006

De Vrieze, J., Saunders, A.M., He, Y., Fang, J., Nielsen, P.H., Verstraete, W., Boon, N., 2015. Ammonia and temperature determine potential clustering in the anaerobic digestion microbiome. Water Res. 75, 312–323. https://doi.org/10.1016/J.WATRES.2015.02.025

Di, H.J., Cameron, K.C., Shen, J.-P., Winefield, C.S., O'Callaghan, M., Bowatte, S., He, J.-Z., 2010. Ammonia-oxidizing bacteria and archaea grow under contrasting soil nitrogen conditions. FEMS Microbiol. Ecol. 72, 386–394. https://doi.org/10.1111/j.1574-6941.2010.00861.x

Escudié, F., Auer, L., Bernard, M., Mariadassou, M., Cauquil, L., Vidal, K., Maman, S., Hernandez-Raquet, G., Combes, S., Pascal, G., 2018. FROGS: Find, Rapidly, OTUs with Galaxy Solution. Bioinformatics 34, 1287–1294. https://doi.org/10.1093/bioinformatics/btx791

Farrow, C., Crolla, A., Kinsley, C., McBean, E., 2017. Ammonia removal from poultry manure leachate via struvite precipitation: A strategy for more efficient anaerobic digestion. Int. J. Environ. Technol. Manag. 20, 87–100. https://doi.org/10.1504/IJETM.2017.086463

Garcia-Peña, E.I., Parameswaran, P., Kang, D.W., Canul-Chan, M., Krajmalnik-Brown, R., 2011. Anaerobic digestion and co-digestion processes of vegetable and fruit residues: Process and microbial ecology. Bioresour. Technol. 102, 9447–9455. https://doi.org/10.1016/J.BIORTECH.2011.07.068

Godon, J.-J., Moriniere, J., Moletta, M., Gaillac, M., Bru, V., Delgenes, J.-P., 2005. Rarity

associated with specific ecological niches in the bacterial world: the “Synergistes” example. Environ. Microbiol. 7, 213–224. https://doi.org/10.1111/j.1462-2920.2004.00693.x

Islam, G.M., Vi, P., Gilbride, K.A., 2019. Functional relationship between ammonia-oxidizing bacteria and ammonia-oxidizing archaea populations in the secondary treatment system of a full-scale municipal wastewater treatment plant. J. Environ. Sci. 86, 120–130. https://doi.org/10.1016/J.JES.2019.04.031

Ito, T., Yoshiguchi, K., Ariesyady, H.D., Okabe, S., 2011. Identification of a novel acetate-utilizing bacterium belonging to Synergistes group 4 in anaerobic digester sludge. ISME J. 5, 1844–1856. https://doi.org/10.1038/ismej.2011.59

Kalamaras, S.D., Vasileiadis, S., Karas, P., Angelidaki, I., Kotsopoulos, T.A., 2020. Microbial adaptation to high ammonia levels during anaerobic digestion of manure-based feedstock; Biomethanation and 16S rRNA gene sequencing. J. Chem. Technol. Biotechnol. jctb.6385. https://doi.org/10.1002/jctb.6385

Könneke, M., Bernhard, A.E., de la Torre, J.R., Walker, C.B., Waterbury, J.B., Stahl, D.A., 2005. Isolation of an autotrophic ammonia-oxidizing marine archaeon. Nature 437, 543–546. https://doi.org/10.1038/nature03911

Lee, S.-H., Park, J.-H., Kim, S.-H., Yu, B.J., Yoon, J.-J., Park, H.-D., 2015. Evidence of syntrophic acetate oxidation by Spirochaetes during anaerobic methane production. Bioresour. Technol. 190, 543–549. https://doi.org/10.1016/j.biortech.2015.02.066

Madigou, C., Poirier, S., Bureau, C., Chapleur, O., 2016. Acclimation strategy to increase phenol tolerance of an anaerobic microbiota. Bioresour. Technol. 216, 77–86. https://doi.org/10.1016/j.biortech.2016.05.045

McMurdie, P.J., Holmes, S., 2013. phyloseq: An R Package for Reproducible Interactive Analysis and Graphics of Microbiome Census Data. PLoS One 8, e61217.

https://doi.org/10.1371/journal.pone.0061217

Ortner, M., Leitzinger, K., Skupien, S., Bochmann, G., Fuchs, W., 2014. Efficient anaerobic mono-digestion of N-rich slaughterhouse waste: Influence of ammonia, temperature and trace elements. Bioresour. Technol. 174, 222–232. https://doi.org/10.1016/j.biortech.2014.10.023

Patel, G.B., MacKenzie, C.R., 1982. Metabolism of Acetivibrio cellulolyticus during optimized growth on glucose, cellobiose and cellulose. Eur. J. Appl. Microbiol. Biotechnol. 16, 212–218. https://doi.org/10.1007/BF00505835

Puig-Castellví, F., Cardona, L., Jouan-Rimbaud Bouveresse, D., Cordella, C.B.Y., Mazéas, L., Rutledge, D.N., Chapleur, O., 2020. Assessment of the microbial interplay during anaerobic co-digestion of wastewater sludge using common components analysis. PLoS One 15, e0232324. https://doi.org/10.1371/journal.pone.0232324

Rajagopal, R., Massé, D.I., Singh, G., 2013. A critical review on inhibition of anaerobic digestion process by excess ammonia. Bioresour. Technol. 143, 632–641. https://doi.org/10.1016/J.BIORTECH.2013.06.030

Rivière, D., Desvignes, V., Pelletier, E., Chaussonnerie, S., Guermazi, S., Weissenbach, J., Li, T., Camacho, P., Sghir, A., 2009. Towards the definition of a core of microorganisms involved in anaerobic digestion of sludge. ISME J. 3, 700–714. https://doi.org/10.1038/ismej.2009.2

Rui, J., Li, J., Zhang, S., Yan, X., Wang, Y., Li, X., 2015. The core populations and co-occurrence patterns of prokaryotic communities in household biogas digesters. Biotechnol. Biofuels 8, 158. https://doi.org/10.1186/s13068-015-0339-3

Rutledge, D.N., 2018. Comparison of Principal Components Analysis, Independent Components Analysis and Common Components Analysis. J. Anal. Test. 2, 235–248. https://doi.org/10.1007/s41664-018-0065-5

Su, X.-L., Tian, Q., Zhang, J., Yuan, X.-Z., Shi, X.-S., Guo, R.-B., Qiu, Y.-L., 2014. Acetobacteroides hydrogenigenes gen. nov., sp. nov., an anaerobic hydrogen-producing bacterium in the family Rikenellaceae isolated from a reed swamp. Int. J. Syst. Evol. Microbiol. 64, 2986–2991. https://doi.org/10.1099/ijs.0.063917-0

Tian, H., Fotidis, I.A., Mancini, E., Treu, L., Mahdy, A., Ballesteros, M., González-Fernández, C., Angelidaki, I., 2018. Acclimation to extremely high ammonia levels in continuous biomethanation process and the associated microbial community dynamics. Bioresour. Technol. 247, 616–623. https://doi.org/10.1016/J.BIORTECH.2017.09.148

Wang, Q., Garrity, G.M., Tiedje, J.M., Cole, J.R., 2007. Naive Bayesian classifier for rapid assignment of rRNA sequences into the new bacterial taxonomy. Appl. Environ. Microbiol. 73, 5261–7. https://doi.org/10.1128/AEM.00062-07

Wang, Y., Qian, P.-Y., 2009. Conservative Fragments in Bacterial 16S rRNA Genes and Primer Design for 16S Ribosomal DNA Amplicons in Metagenomic Studies. PLoS One 4, e7401. https://doi.org/10.1371/journal.pone.0007401

Whiticar, M.J., Faber, E., Schoell, M., 1986. Biogenic methane formation in marine and freshwater environments: CO2reduction vs. acetate fermentation-Isotope evidence. Geochim. Cosmochim. Acta 50, 693–709. https://doi.org/10.1016/0016-7037(86)90346-7

Wittmann, C., Zeng, A.-P., Deckwer, W.-D., 1995. Growth inhibition by ammonia and use of a pH-controlled feeding strategy for the effective cultivation of Mycobacterium chlorophenolicum. Appl. Microbiol. Biotechnol. 44, 519–525. https://doi.org/10.1007/BF00169954

Yan, M., Fotidis, I.A., Tian, H., Khoshnevisan, B., Treu, L., Tsapekos, P., Angelidaki, I., 2019. Acclimatization contributes to stable anaerobic digestion of organic fraction of municipal solid waste under extreme ammonia levels: Focusing on microbial community

dynamics. Bioresour. Technol. 286, 121376.
https://doi.org/10.1016/j.biortech.2019.121376

Yenigün, O., Demirel, B., 2013. Ammonia inhibition in anaerobic digestion: A review. Process Biochem. 48, 901–911. https://doi.org/10.1016/J.PROCBIO.2013.04.012

Figure 1. Summary of the performance data. Vertical blue lines correspond to the start of the NH_3 addition. The two parallel lines of the same color as the reactor labels denote the limits of the plateau period at the highest NH_3 concentration. Horizontal black lines in the apparent isotopic factor (α_{app}) indicate the thresholds limits for the methanogenic acetoclastic (α_{app}<1.055) or hydrogenotrophic (α_{app}>1.065) activities in the digesters.

Figure 2. Microbial structure of the reactors. **A)** Relative abundance of archaea. **B)** Relative abundance of bacteria. Black lines in **A)** represent the NH_3 concentration over time in the reactor.

Figure 3. Heatmap representation of the reactors' evolution over time. **A-C)** Common Components Analysis scores. **D)** TAN. **E)** pH. **F)** Apparent isotopic factor (α_{app}). In **F)**, Samples with a hydrogenotrophic methanogenic profile (α_{app} > 1.065) were labelled with 'h', while those with a marked acetoclastic methanogenic profile (α_{app} < 1.055) were labelled with 'a'. Red dashed lines represent the limits of the plateau period at the highest NH_3 concentration, while the black dashed lines represent the acclimation and restoration periods.

Figure 4. Interpretation of CCA results.

Figure 5. Phylogenetic tree of the OTUs selected from the CCA analysis. OTUs, represented by the outer dots in the tree, were colored differently according to the component they were selected in: red for OTUs selected in CC1, blue for OTUs selected in CC2, and green for OTUs selected in CC3. To improve tree readability, the background of groups of OTUs at different phylogenetic levels were colored according to their average importance of the components (i.e. redder if CC1 is more important, and so on). Full phylogenetic affiliation associated with each cluster is given in **Table S1**.

Figures:

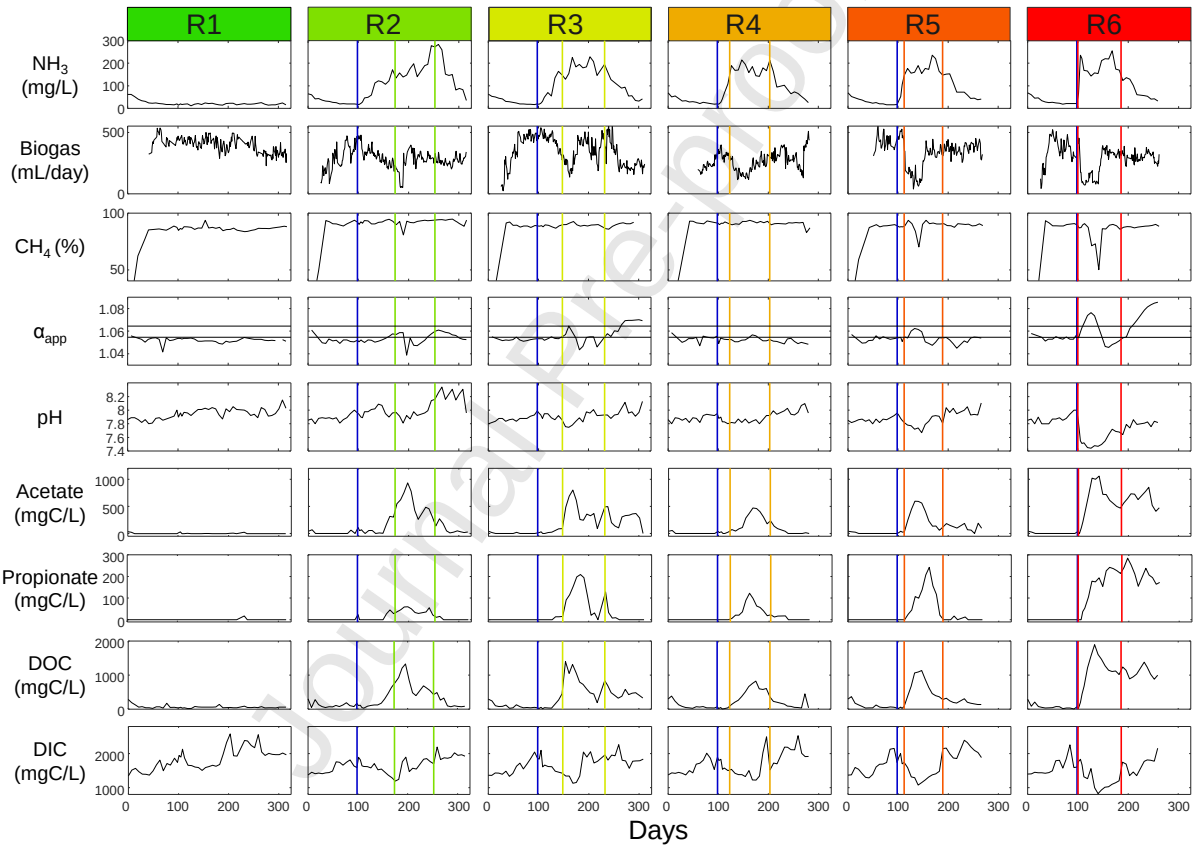

Figure 1

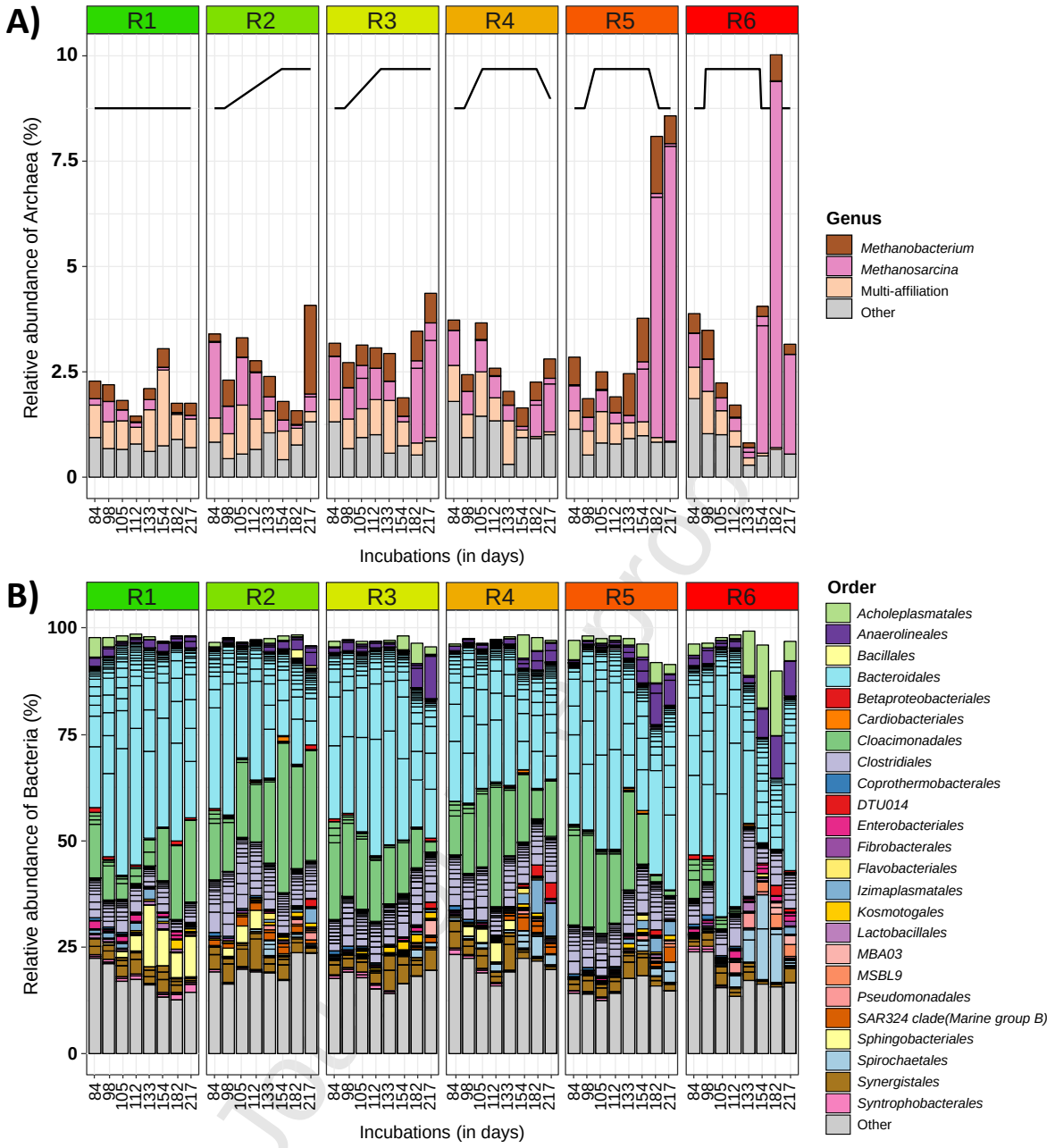
A)
R1
R2
R3
R4
R5
R6
Relative abundance of Archaea (%)
10
7.5
5
2.5
0
84 98 105 112 133 154 182 217
Incubations (in days)
Genus
Methanobacterium
Methanosarcina
Multi-affiliation
Other
B)
Relative abundance of Bacteria (%)
100
75
50
25
0
Order
Acholeplasmatales
Anaerolineales
Bacillales
Bacteroidales
Betaproteobacteriales
Cardiobacteriales
Cloacimonadales
Clostridiales
Coprothermobacterales
DTU014
Enterobacteriales
Fibrobacterales
Flavobacteriales
Izimaplasmatales
Kosmotogales
Lactobacillales
MBA03
MSBL9
Pseudomonadales
SAR324 clade(Marine group B)
Sphingobacteriales
Spirochaetales
Synergistales
Syntrophobacterales
Other

Figure 2

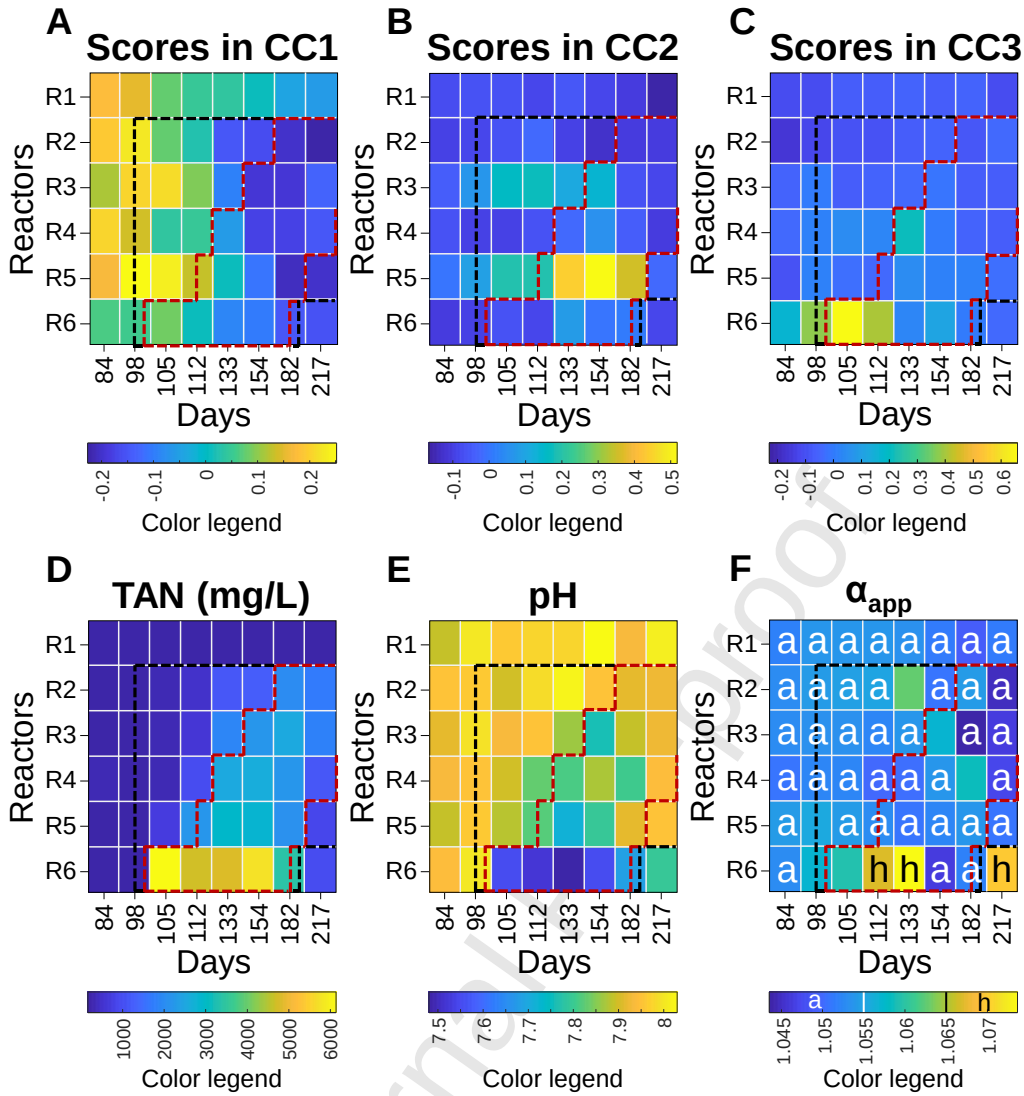

Figure 3

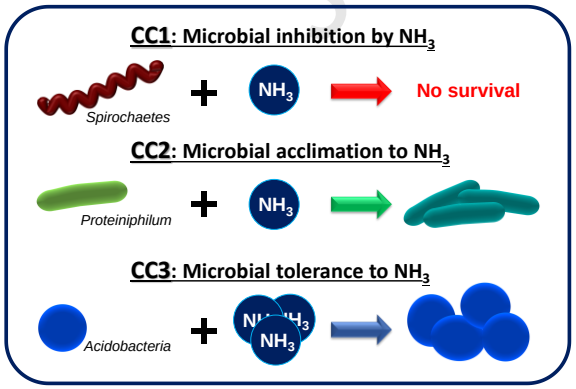

Figure 4

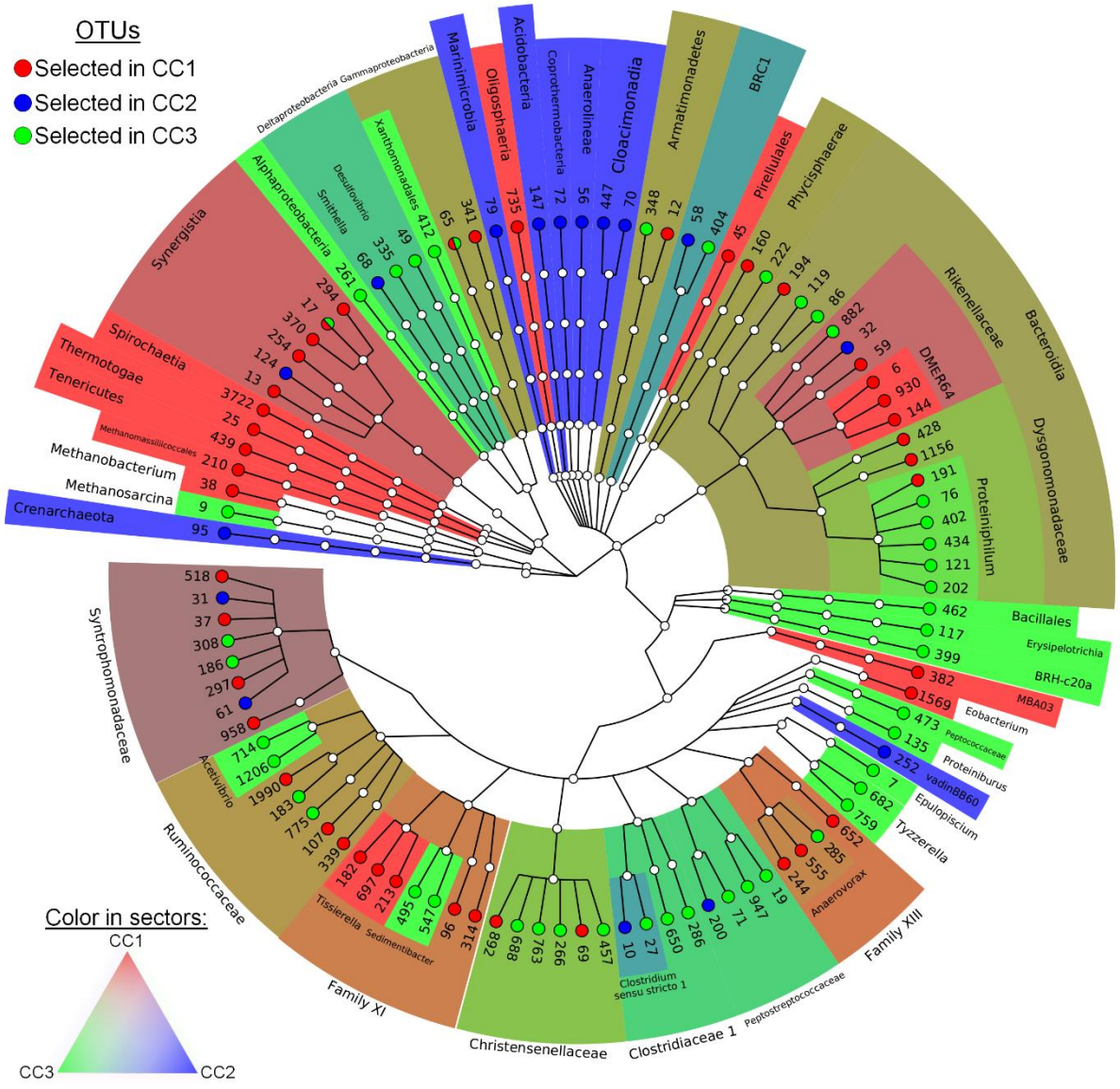
OTUs
Selected in CC1
Selected in CC2
Selected in CC3
Color in sectors:
CC1
CC3
CC2
Deltaproteobacteria
Gammaproteobacteria
Alphaproteobacteria
Marinimicrobia
Oligosphaeria
Acidobacteria
Coprothermobacteria
Anaerolineae
Cloacimonadia
Armatimonadetes
BRC1
Pirellulales
Phycisphaerae
Bacteroidia
Rikenellaceae
Dysgonomonadaceae
DMER64
Proteiniphilum
Bacillales
Erysipelotrichia
BRH-c20a
MBA03
Eobacterium
Peptococcaceae
Proteiniborus
vadinBB60
Epulopiscium
Tyzzerella
Anaerovorax
Family XIII
Peptostreptococcaceae
Clostridiaceae 1
Clostridium sensu stricto 1
Christensenellaceae
Family XI
Tissierella
Sedimentibacter
Ruminococcaceae
Acetivibrio
Syntrophomonadaceae
Synergistia
Spirochaetia
Thermotogae
Tenericutes
Methanomassiliicoccales
Methanobacterium
Methanosarcina
Crenarchaeota
Xanthomonadales
Desulfovibrio
Smithella

Figure 5

Declaration of interests

☒ The authors declare that they have no known competing financial interests or personal relationships that could have appeared to influence the work reported in this paper.

☐The authors declare the following financial interests/personal relationships which may be considered as potential competing interests:

Graphical abstract

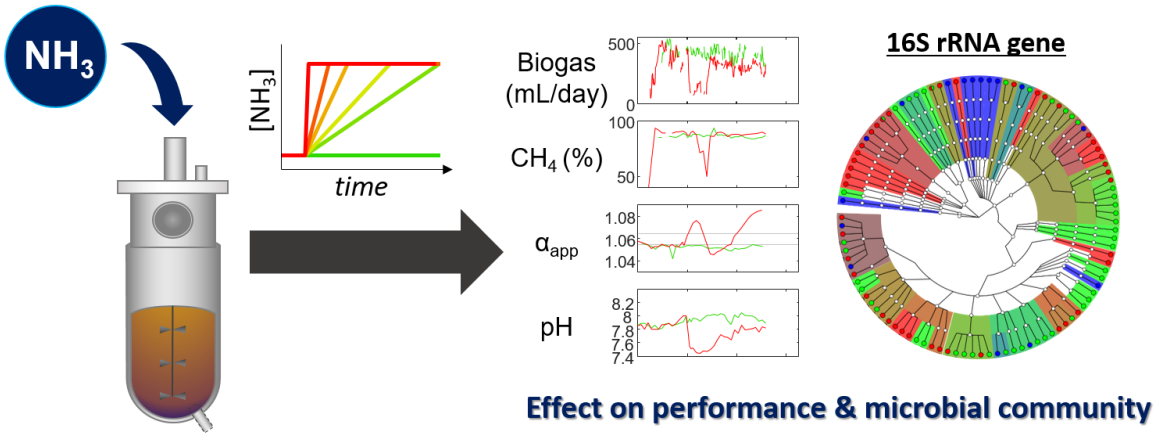

Highlights:

- The influence of different NH_3 loading rates in AD acclimation was tested.
- All tested acclimation strategies altered the digesters states.
- The most affected parameters were the VFA and the biogas production.
- The microbial communities were modulated by the NH_3 loading rate.
- Most of the acclimated OTUs are from the *Clostridiales* and *bacteroidales* orders.